Journal of Structural Geology, Vol. 3, No. 3, pp. 279 to 290, 1981.
Printed in Great Britain

0191-8141/81/030279-11 $02.00/0
Pergamon Press Ltd.

A microstructural and microchemical study of cleavage lamellae in a slate

S. H. WHITE and D. C. JOHNSTON

Geology Department, Imperial College, London SW7 2BP, England

(*Received* 11 *October* 1980; *accepted in revised form* 22 *June* 1981)

Abstract—The results of a detailed microstructural and microchemical study of a slate from the Chewton area, Victoria, Australia are reported in which it was found that cleavage developed from microcrenulations. Phyllosilicates in P-domains differed in their chemistry from those in Q-domains and were concentrated in the P-domains by localized metamorphic reactions which were aided by mechanical rotation and solution processes. Wide, dark cleavage lamellae, often taken as evidence for the passive concentration of insoluble minerals, appear to have had a similar origin. The P-domains exhibited two types of microstructure, one which was consistent with annealing and the other with deformation within the domain. Cataclasites had formed along some P-domains, suggesting that they had become preferential sites for late phase brittle deformation.

INTRODUCTION

RECENT TEM (Knipe & White 1977, White & Knipe 1978, Knipe 1979) studies have greatly enhanced our understanding of the processes which contribute to the formation of slaty cleavage in rocks. In the slates studied by this technique it has been found that two processes contribute to cleavage development; crystallisation and mechanical rotation. The former was found to be dominant in the hinge areas of folds and the latter in the limbs, with the siting of the P-domains (phyllosilicate-rich domains) and their initial spacing being controlled by microcrenulations. The initial studies of White & Knipe (1978) concluded that the *P*-domains in some slates were zones of localized metamorphic reactions with solution processes contributing to these, the overall effect being the preferential, but not exclusive, concentration of phyllosilicates in the P-domains. This postulate has now been confirmed in a number of recent studies (Beach 1979, Knipe 1979, Stephens *et al.* 1979). The above results indicate that the dark, abnormally wide P-domains seen in some slates and regarded as indicative of the passive concentration of insoluble material by pressure solution (solution transfer) processes (Geiser 1975, Groshong 1975, Bayly *et al.* 1977) may also be zones of metamorphic reaction. In this short paper we present the results of a detailed microstructural and microchemical study of the phyllosilicates in P- and Q-domains in a slate from Wattle Gully, Victoria, Australia.

SLATE SELECTED

The sample studied came from core material from the Wattle Gully Gold Mine near Chewton, central Victoria, which is situated in Lower Ordovician greywackes, siltstones and shales which have developed a slaty cleavage. The area is within the extensive S.E. Australian slate belt. The structural geology and tectonics of the Victorian portion of the belt have been summarized by Beavis (1976). Briefly, a lower Ordovician turbidite sequence has been subjected to a single phase of folding which has resulted in anticlinoria and synclinoria comprised of tight, upright folds. Detailed optical and geochemical studies of similar, low grade slates from a nearby area (Clunes) within the belt have been published by Glasson & Keays (1978) and by Stephens *et al.* (1979).

Core material provided fresh samples which are difficult to obtain in this slate belt because of deep weathering.

EXPERIMENTAL TECHNIQUES

Preparation techniques employed the same procedure as described by White & Knipe (1978). Detailed optical studies were performed on ultra-thin sections ($\simeq 5\,\mu$m thick). Detailed microstructural studies were undertaken on an AEI EM7 high voltage transmission electron microscope, operating at 1000 KV.

A Jeol 120CX STEM fitted with a Link energy-dispersive X-ray system was used for micro-analytical studies. This relatively new technique enables quantitative analyses to be obtained from very small grains ($< 0.1\,\mu$m diameter) in specimens which are thin enough to be examined microscopically by a 100 KV TEM. Determination of elemental concentrations involved the calculation of weight fraction ratios of two elements by relating the background-corrected characteristic X-ray intensities to an experimentally derived constant, K, by the expression

$$\frac{I_A}{I_B} = K\frac{C_A}{C_B}$$

where I_A and I_B are the X-ray intensities and C_A and C_B are the weight fractions of the two elements A and B (see Lorrimer *et al.* 1973, Cliff & Lorrimer 1975). The value of K was determined by measurements on standards of known composition and all ratios were taken with respect to a single element, namely Si. The above calculation is

Table 1. Comparison between wet chemical analysis of a standard mica and STEM analysis

	1 Wet chemistry % oxide	2 Wet chemistry (recalculated) % oxide	3 Stem % oxide
Na	0.98	1.03	0.36
Mg	0.83	0.88	1.13
Al	31.80	33.55	33.87
Si	46.30	48.85	49.46
K	10.60	11.18	10.92
Ca	0.13	0.14	0.00
Ti	0.46	0.49	0.46
Fe	3.68	3.88	3.81
H_2O	5.30		

strictly valid only for infinitely thin foils where primary X-rays are neither absorbed nor excite fluorescent radiation. In practice, however, it was found that the finite thickness of the specimen resulted in a reduction in intensity of the low-energy X-ray peaks (see also Knipe 1979) but by assuming a uniform ionization density with depth, absorption correction factors are included in the computation program which utilize X-ray take-off angle, the thickness and density of the specimen and the mean mass absorption coefficient of the element under consideration. Despite these correction factors, however, accurate detection of small amounts of Na proved to be a recurring problem, although not one which substantially altered the major results of this study. We found no evidence, however, of diffusion of volatile elements away from the analysed spot (see Knipe 1979, Craw 1981). The specimen thickness was determined by tilting to a known amount after analysis and measuring the lateral displacement of the contamination marks on the top and bottom of the foil (see Goodhew & Chescoe 1980).

Accuracy of chemical analyses and hardware stability were tested during each analysis session by reference to a standard mica, the composition of which was known accurately through wet chemistry (provided by Dr. R. J. Knipe). This wet chemical analysis, together with a typical STEM analysis is shown in Table 1. For comparison, column 2 shows the wet chemical analysis with H_2O subtracted and recalculated to 100%. These results show good correlation between the two methods, particularly for those elements which occur in significant amounts (Al, Si, K, Ti and Fe).

RESULTS

The overall microstructure of the slate studied is shown in Fig. 1. This slate consisted of alternating bands of pelitic and silty layers with a well developed cleavage marked by narrow dark P-domains in the pelitic layers. In the vicinity of the hinge areas of the folds several P-domains coalesced to eventually form a single, very dark, wide P-domain which in instances cut through the silty layers. Lateral displacement of the silty layers across some of these opaque P-domains was common (Fig. 1).

Detailed optical studies were carried out on ultra-thin ($<10\,\mu m$) petrological sections (Figs. 2 and 3). The P-domains became transparent as the thickness of the section was reduced, suggesting that the darkness is the result of staining. There appeared to be fewer opaques in the P-domains than in some of the Q-domains (quartz rich) and this was subsequently confirmed by electron microscopy. The detailed studies revealed that the P-domains marked the axial planes of a microcrenulation cleavage (Fig. 2a). Narrow, non-penetrative, incipient P-domains occurred within the Q-domains (Figs. 2b & c). However, as the Q-domains narrowed adjacent to the silty layers, the non-penetrative P-domains became penetrative, i.e. coalescence occurred by the continued widening and development of the narrow non-penetrative domains (Fig. 2d). The anastomosing nature of the P-domains is clearly seen in Fig. 2(d). The manner in which anastomosing occurred often gave the appearance of a second weak foliation at a slight angle to the main slaty cleavage. No meaningful information on the microstructure of the P-domains could be obtained from the optical studies apart from the occasional recognition of small chlorite and mica grains.

The Q-domains consisted mainly of chlorite, mica and quartz with small amounts of albite and carbonate. Chlorite pods were present in about 10% of the Q-domains. The pods had within them interleaved micas. Most pods showed evidence of deformation, mainly bending of the grains (Fig. 2a). In some, both straight and bent phyllosilicates coexisted, indicating that growth of the chlorite domains had occurred during cleavage development. The quartz grains on the other hand showed no evidence of internal deformation, i.e. they had straight extinction.

The quartz grains in the silty layers also showed straight extinction. Some silty layers contained fine pelitic bands. Their micas and chlorites showed a well-preserved bedding fabric (Fig. 3) and were slightly crenulated. It is a reasonable assumption that the original bedding fabrics of the phyllosilicates in the pelites resembled the above.

The microcrenulation cleavage in the slates was more easily seen in low magnification transmission electron micrographs than in optical micrographs (Fig. 4a). The P- and Q-domains were easily distinguished. The deformation of the phyllosilicates in the Q-domains was much more complex than indicated by optical examination and was mainly due to grain-to-grain interference between adjacent phyllosilicates and quartz grains. Also, more incipient P-domains were seen in electron micrographs, the reason being that many were less than 1 μm wide and were therefore not resolved in an optical microscope. Some of these were seen (in electron micrographs) in the slate adjacent to the silty layers. Individual grains developing along the axial planes of isolated kinked phyllosilicates were also seen (e.g. ringed area in Fig. 4b). Consequently, the Q-domains contain a mixture of both deformed and recrystallized grains. Dislocation structures similar to that shown in Fig. 4(c) were observed in many quartz grains in the Q-domains. This type of radiating structure is typical of that found in quartz overgrowths (Grant & White 1978) and it is suggested that these have a

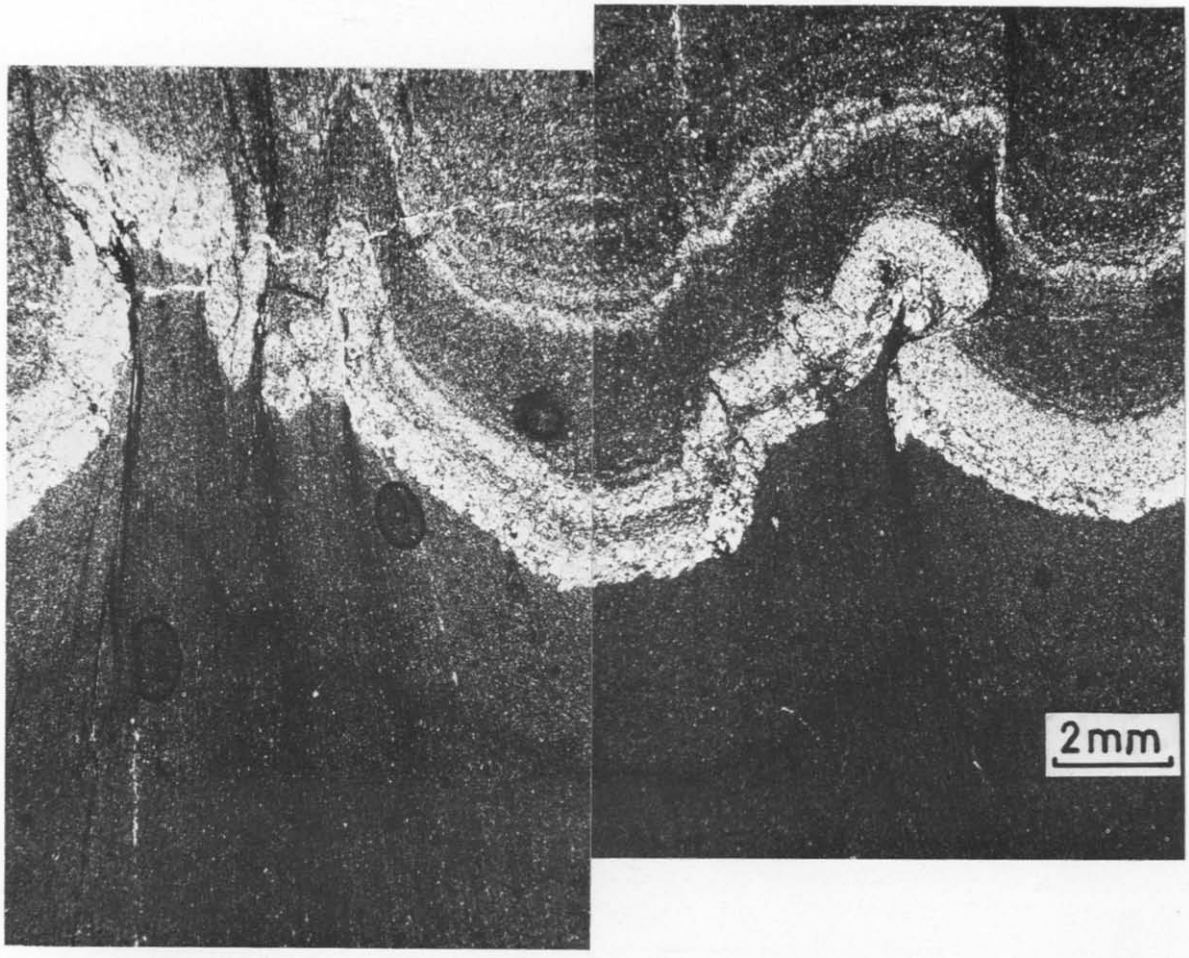

Fig. 1. Optical micrograph of the slate studied. This shows the microfolding in the silty layer. Wide dark P-domains are evident and cut through the silty layers. Dark rimmed elliptical areas are bubbles in the slide.

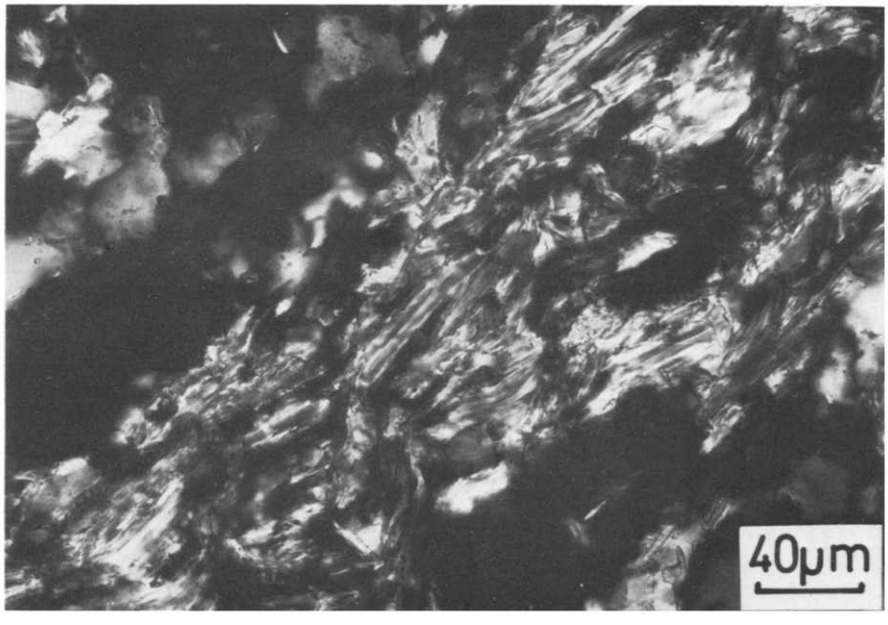

Fig. 3. Optical micrograph showing the bedding fabric in a narrow pelitic seam in a silty layer.

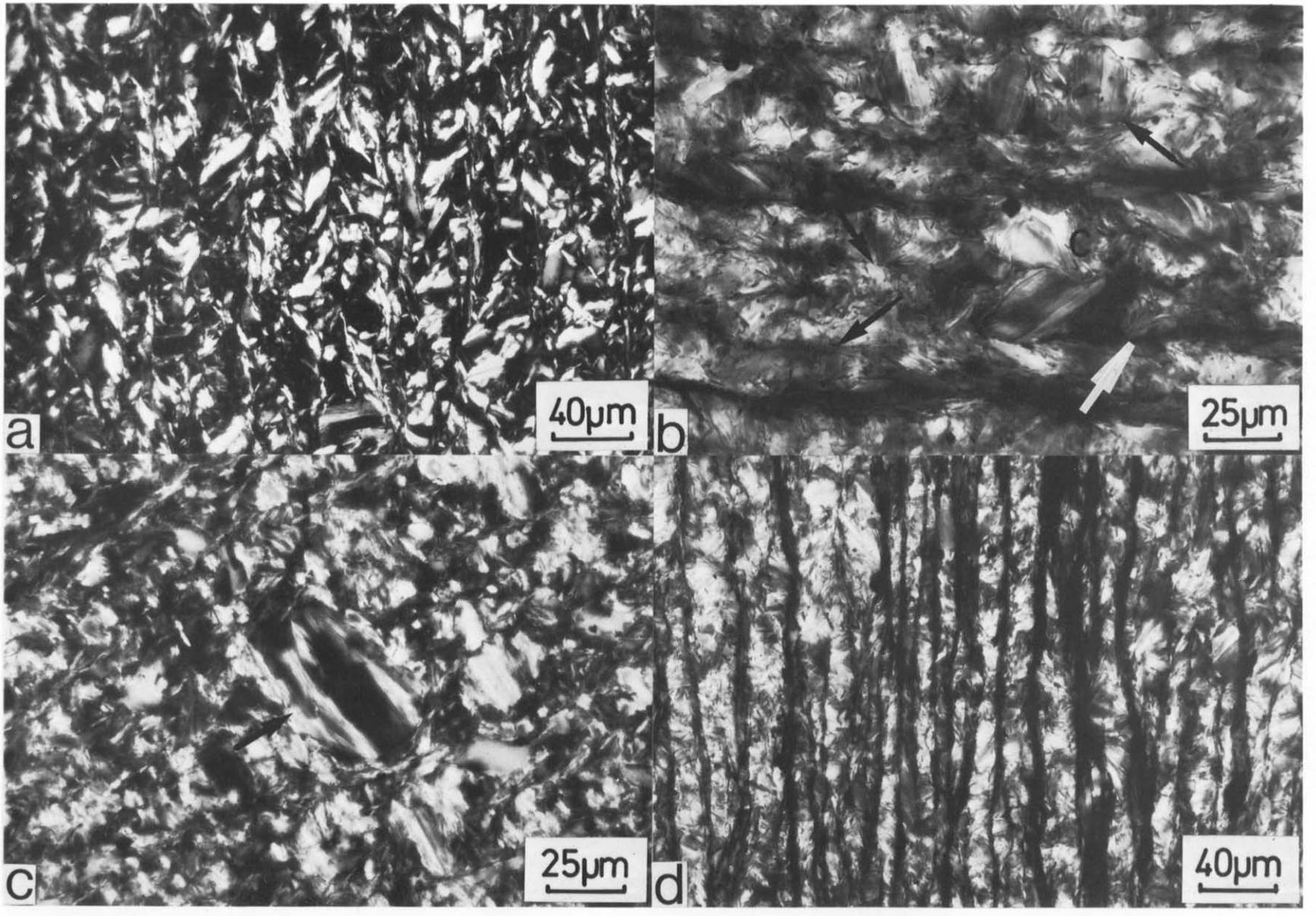

Fig. 2. Optical micrographs of the slate studied showing well-developed P- and Q-domains. (a) A micrograph from an ultra thin section showing the localization of the P-domains along the axial planes of microcrenulations. This microstructure is typical of areas away from the silty layers. (b) Details of the microstructure in Q-domains. A crenulated chlorite grain marked, c, and incipient P-domains, arrowed can be seen. (c) A chlorite pod, arrowed, in a Q-domain. It can be seen to consist of both straight (central part) and bent grains (outer parts). Incipient P-domains can also be seen. (d) Typical microstructure in the slate adjacent to the silicity layers. Anastomosing of the dark P-domains is clearly visible. Normal thin section.

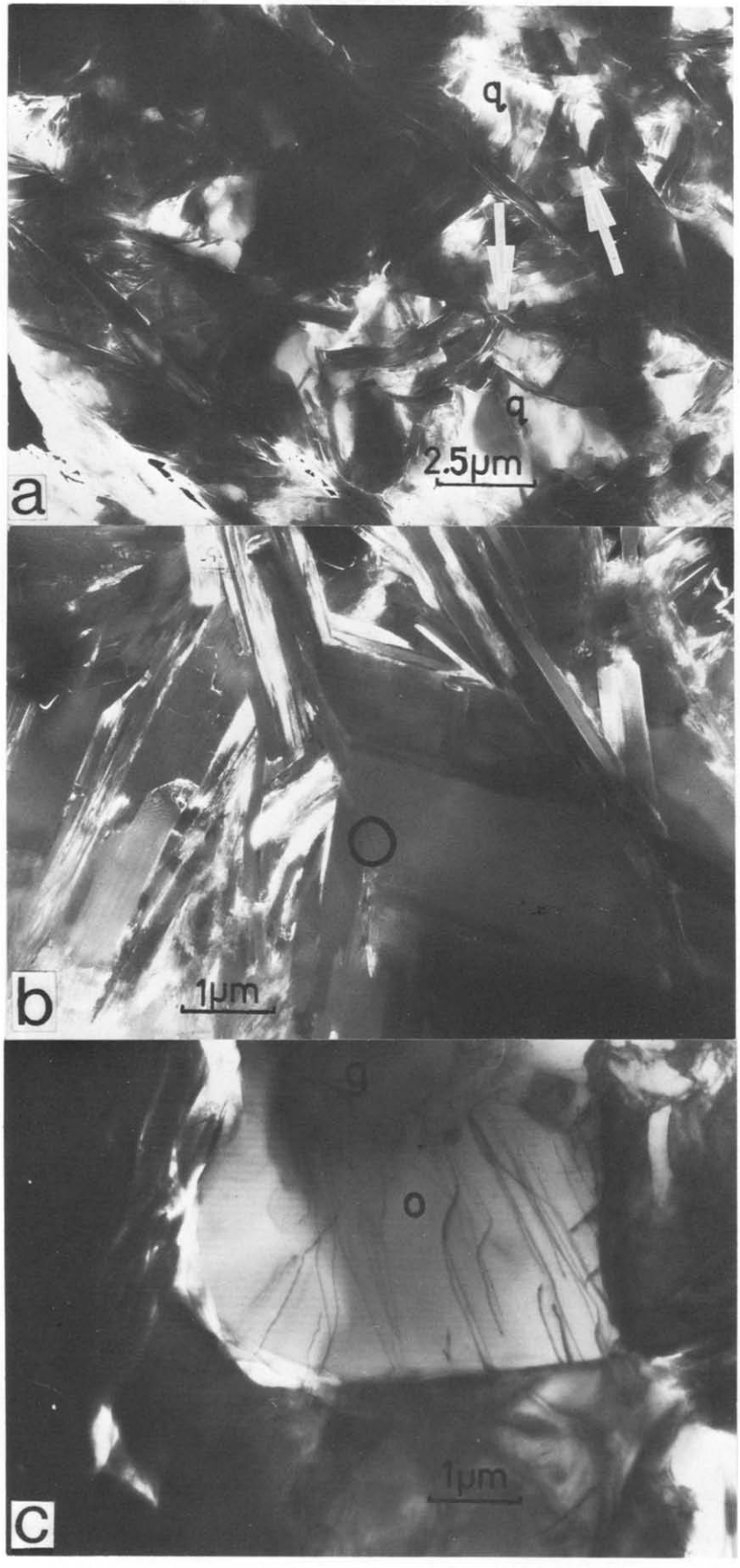

Fig. 4. Dark field electron micrographs depicting the typical slate microstructure in areas corresponding to those shown in Fig. 2(a). The P-domains and Q-domains (q) are clearly seen in (a). Incipient P-domains are arrowed. The relationship between the cleavage and microcrenulations is best seen in the Q-domains (b). Also note, in (b), the difference in grain size between the phyllosilicates in the P-domains and the adjacent Q-domains. (c) shows a quartz overgrowth, O, marked by radiating dislocations, on a small quartz grain, g, in a Q-domain.

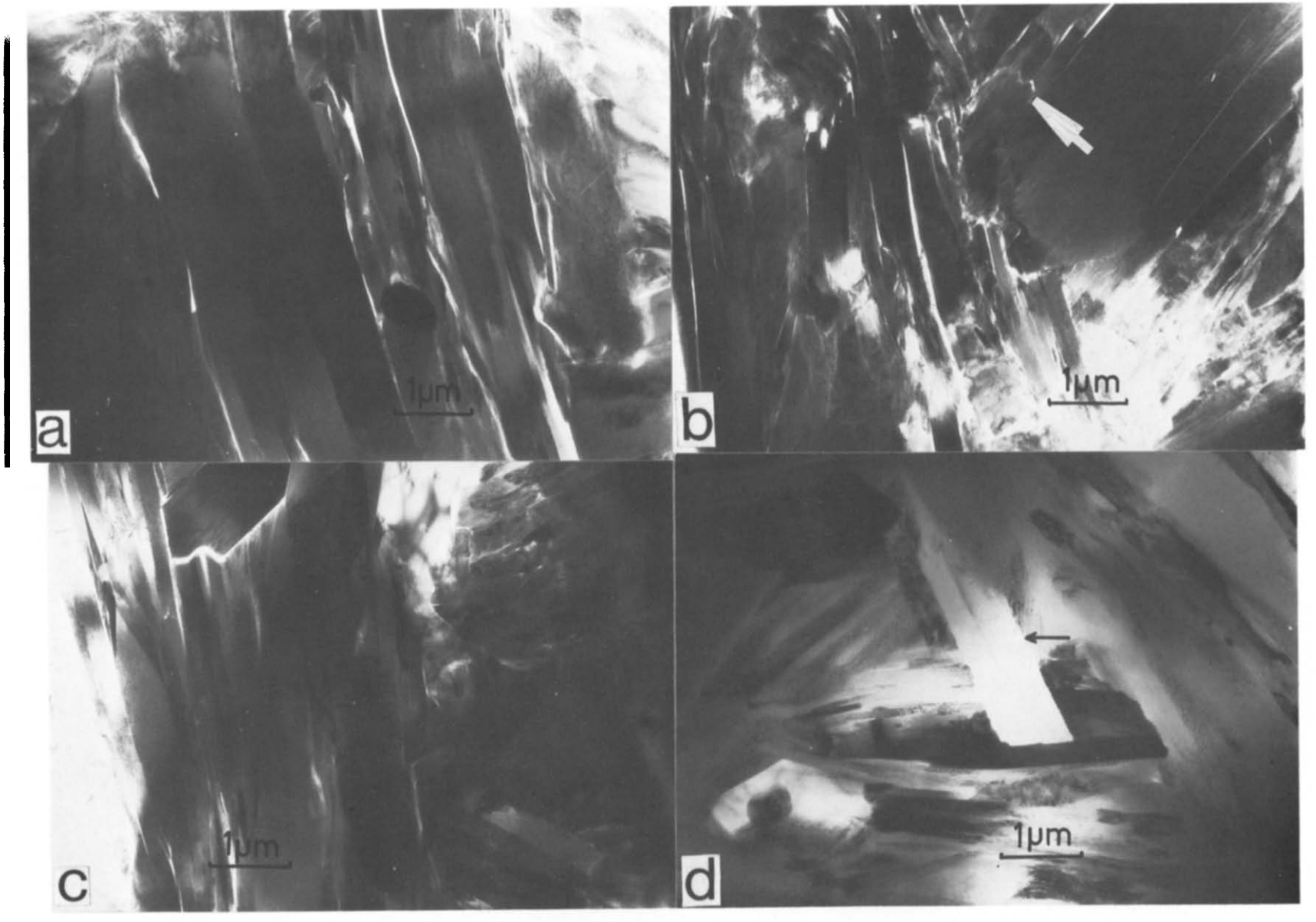

Fig. 5. Bright field electron micrographs showing details of the P-domains. The phyllosilicates in some domains showed evidence of deformation which ranged from slight (a), to pronounced, (b). Those in other domains exhibited an annealed texture (c and d). The latter were characterized by grains growing across P-domains (c) and across P- and Q-domain interfaces (arrowed grain in d) Note the difference in the interfaces between the deformed (b) and annealed P-domains (c and d). The opaque grain in (a) is a rutile.

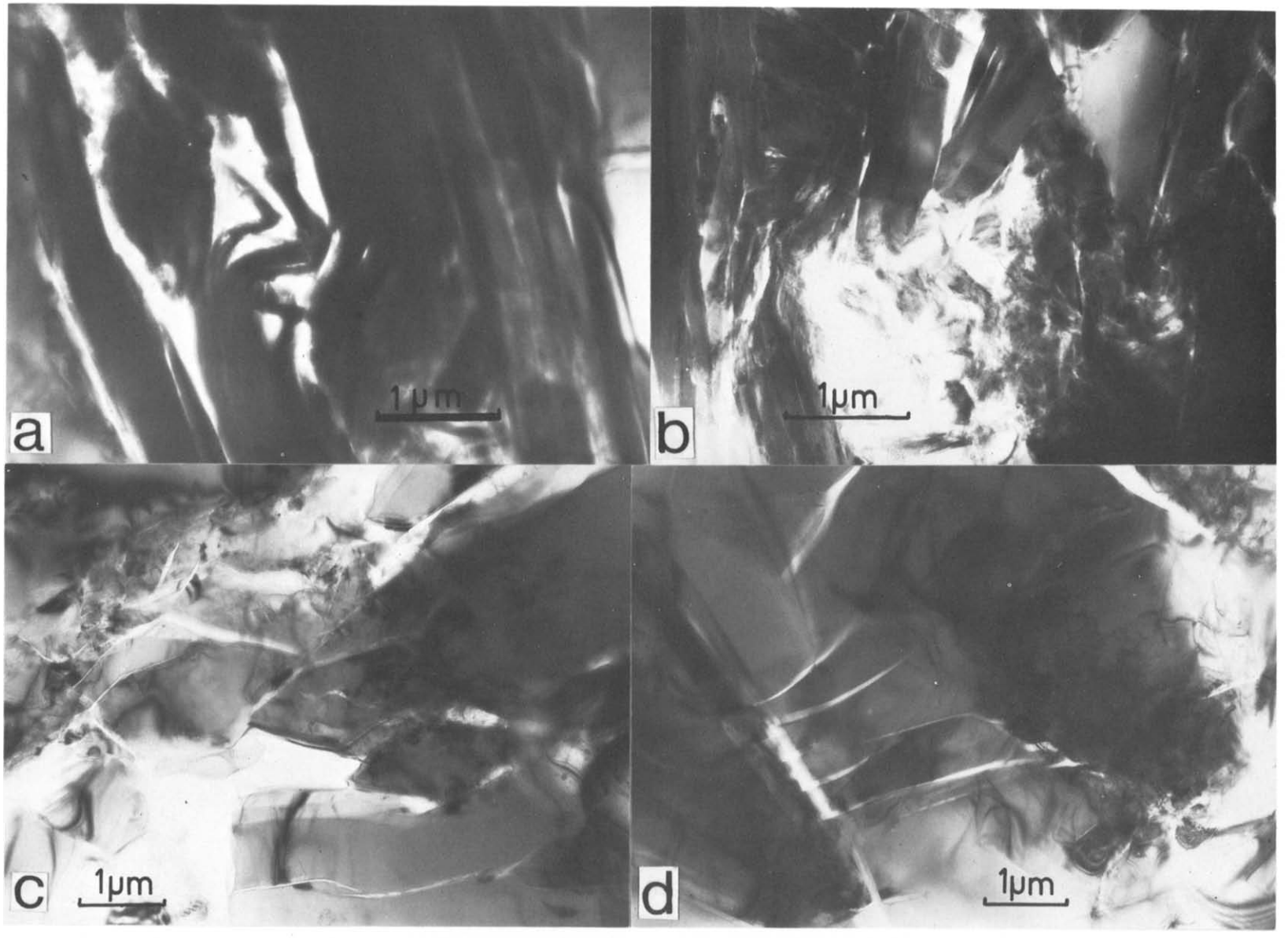

Fig. 6. Bright field electron micrographs from the P-domains shown in Fig. 2(d). They were characterized by deformed chlorite and mica grains (a) which in the vicinity of the silty layers became broken up (b). The deformation of the phyllosilicate grains was variable across the P-domains, with some grains displaying intra-folial bending (a). Adjacent to the silty layers the P-domains contained broken pieces of quartz (c) while the quartz grains within the silty layers were extensively fractured (d). Note the lack of dislocations in the fractured quartz grains indicating that the grains were not ductile prior to fracturing. Also note the absence of corrosion along the fractures.

similar origin; that being so, overgrowths were commonly encountered on Q-domain quartz grains.

Most attention, during electron microscopy, was paid to the microstructure of P-domains, especially microstructural variations associated with the coalescence and darkening of these domains adjacent to the folds in the silty layers. Typical microstructures are shown in Figs. 4 and 5. Close inspection of these figures show that two distinct microstructural types of P-domains occur and shall be referred to as deformed (Figs. 5a & b) and annealed (Figs. 5c & d) textural types. In the deformed type all of the phyllosilicate grains were aligned approximately parallel to the P-domain edges. Apart from the narrow P-domains of this type, the phyllosilicate grains showed evidence of bending. Large detrital phyllosilicates adjacent to these P-domains tended to have a jagged abutment with the domains (e.g. the large grain in 5b). A fine-grained film of phyllosilicates occurred at the edges of some of these domains. On the other hand, the annealed type P-domains, with a texture similar to that described by Oertal & Phakey (1972), contained straight (unbent) phyllosilicate laths, the majority of which were parallel to the domain edges but some of which were at a high angle to the edge (see Figs. 4b, 5c & d). The contacts between the P- and Q-domains also differed from the deformed type. They were sharp with P- and Q-domain phyllosilicate grains growing across the borders (see arrowed areas in Figs. 4b and 5d). Small grains of quartz occurred in both types of P-domains as did small opaques (identified in STEM as titanium oxides). Lamellae entirely contained within a single Q-domain were always of the annealed type; those which were penetrative were of both types, with a tendency for the widest ($\gg 1$ μm wide) to be of the deformed type.

The wide dark P-domains adjacent to the silty layers were all of the deformed type. The deformation within them was much more pronounced than that in the P-domains away from the silty layers. The phyllosilicates became fractured, bent and twisted and some were shredded (Fig. 6a & b). They also contained angular fragments of quartz (Fig. 6c). The quartz in the silty layers adjacent to the penetrative P-domains was fractured (Fig. 6d). The microstructure of these P-domains resembled that of cataclasites. There is supporting microstructural evidence that sliding had occurred along these domains, the most convincing being the localized 'intrafolial' bending of phyllosilicate grains (Fig. 6a).

MICROANALYSIS

The results of the microanalysis of the sheet silicates present are summarized in Fig. 7. Figure 7(a) shows that mica crystals within P-domains tended to be more phengitic than those in the Q-domains, i.e. increased substitution by Mg^{2+} and Fe^{2+} of Al^{VI} ions accompanied by substitution of Al^{IV} by Si^{3+}. The two groups were not totally distinct chemically, there being a shared field in which crystals of similar compositions occur. These results compare favourably with those obtained by Knipe (1979) for the Rhosneigr slate. Analyses of micas in the fine-grained border areas of the P-domains are not recorded on this diagram, as they invariably plotted within the overlapping compositional field. When plotted on an AFN diagram (Fig. 7b) no distinct chemical differences are apparent between the two groups, although this may be due to the low percentages of Na present in the micas and the resulting detection problems of the STEM hardware. The muscovite–phengitic substitution is also clearly seen in Fig. 7(c) where the compositions of the micas in the P-domains (dots) and Q-domains (crosses) have been re-calculated in terms of three theoretical end-member components; phengite, mica and pyrophyllite (see Stephens *et al.* 1979). Chlorite grains tended to be more abundant in the Q-domains and compositionally these plotted in a narrow field (Fig. 7d). The relatively few chlorites analysed from the centres of P-domains indicated a tendency for these to be more Al-rich and less Fe-rich than grains in the Q-domains. The opaque grains in the electron micrographs were found to be rutiles.

DISCUSSION

Cleavage development

The microstructural studies indicate that the cleavage in the slate studied developed mainly by crystallization processes which accompanied the development of a crenulation cleavage, the overall texture being similar to that described as a discrete crenulation cleavage by Gray (1977). The stages in the development of the cleavage, i.e. of the P-domains, could be seen in the wider Q-domains occurring in areas remote from the silty layers. The initial stage of re-orientation involved the kinking and flexuring of the phyllosilicates which resulted in micro-crenulations. These mechanical processes, however, did not completely re-orientate the phyllosilicates and this was achieved by subsequent crystallization of new phyllosilicates along the axial planes of the crenulations. This is the same sequence of processes as reported in the Rhosneigr slates for phyllosilicate re-orientation at the hinge of a fold. The newly crystallized phyllosilicates subsequently grew lengthways into each other to give strands of narrow P-domains, some of which then coalesced to form the penetrative, anastomosing P-domains which mark the slaty cleavage. These subsequently widened by lateral growth and by coalescence with adjacent strands of P-domains. New P-domains were continually developing in the Q-domains because of the continuing imposed deformation on the rock as a whole.

As in the Rhosneigr slate the role of pressure solution processes appears to be subordinate to the mechanical and crystallization processes. Pressure solution would certainly aid the transport of ions required for crystallization and the removal of quartz from the lateral growth front of the widening P-domains. The presence of the overgrowths on the quartz grains suggests that pressure solution processes first concentrated the mobilized quartz

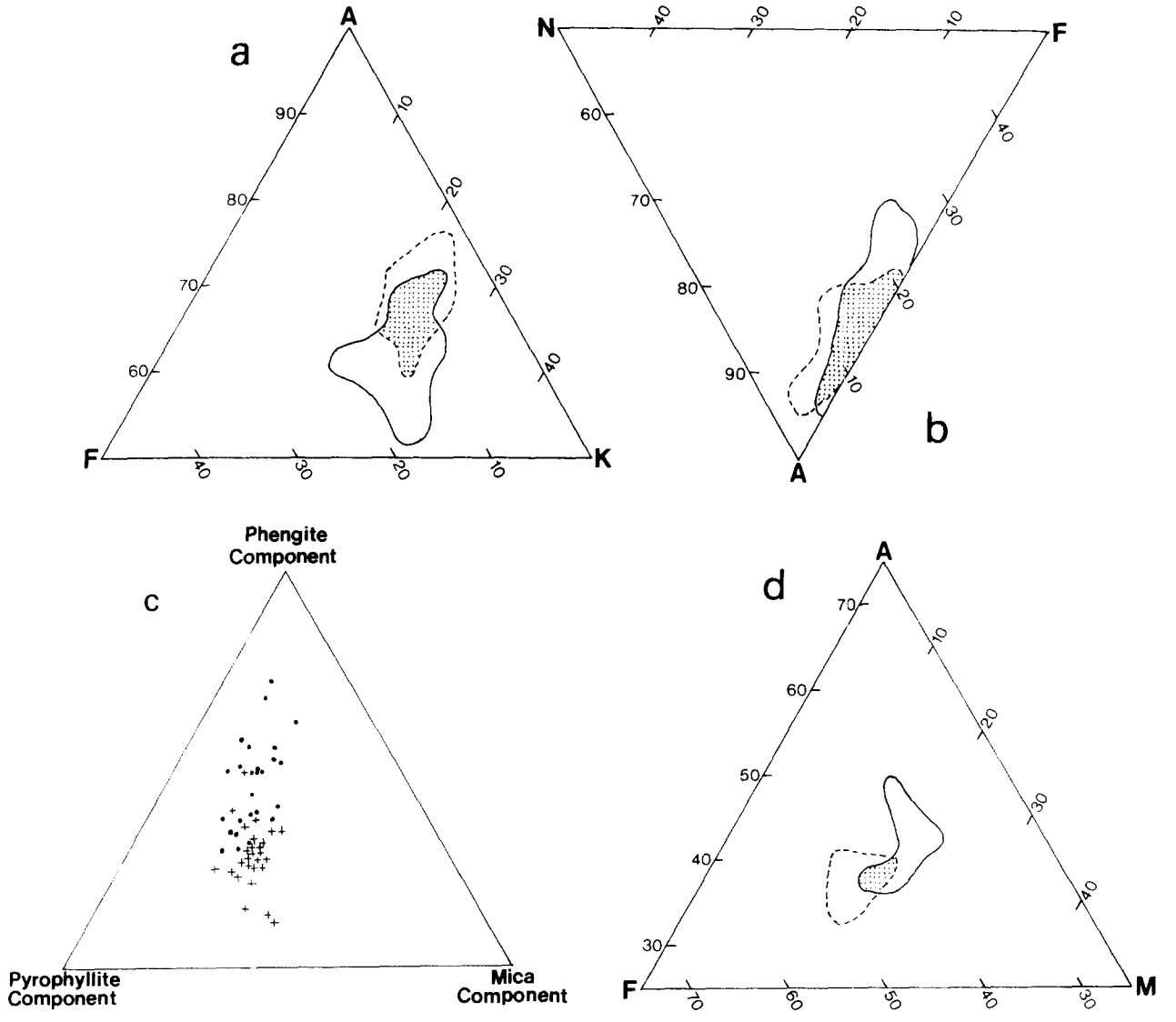

Fig. 7. Chemistry of the sheet silicates. (a) & (b) Compositional fields of micas from Q-domains (broken lines) and P-domains (solid lines). Areas of compositional overlap are stippled. A = Al_2O_3/SiO_2F = FeO + MgO/SiO_2, K = K_2O/SiO_2, N = Na_2O/SiO_2. A + F + K = 100.A + F + N = 100. (c) Compositions of Q-domain micas (crosses) and P-domain micas (dots) expressed in terms of three end-member components: Phengite, $K_2(Fe, Mg, Mn)_2Al_2Si_8O_{20}(OH)_4$, Mica, $K_4Al_4Si_4Al_4)O_{20}(OH)_4$ and Pyrophyllite, $Al_4Si_8O_{20}(OH)_4$ (d) Compositional fields of Q-domain chlorites (broken lines) and P-domain chlorites (solid lines). A = Al_2O_3/SiO_2, F = FeO/SiO_2, MgO/SiO_2. A + F + M = 100.

in the Q-domains before eventually removing it from the immediate system to enable P-domain widening. However, some of the overgrowths may equally have developed during the formation of the crenulation cleavage which preceded the slaty cleavage formation. The control of the shape of the quartz grains by the deformed phyllosilicates in the Q-domains indicates that the overgrowths, or the majority of them, are not remnants of diagenetic processes.

The packing of the phyllosilicate grains in the P-domains is much tighter than in the Q-domains. In the latter areas, pores are seen to form where the phyllosilicates are bent, where they interfere with each other and especially where deformed phyllosilicates abut against the P-domains. This suggests that fluid flow would preferentially be concentrated in the Q-domains, especially at the junction between the P- and Q-domains. There is no evidence that dislocation processes contributed to the deformation, even of the quartz grains. The two types of microstructures in the P-domains can be accounted for by considering the likelihood that shearing (sliding) occurred along some domains but not others. As Williams (1967) pointed out, it is unlikely that P-domains will be precisely parallel to a principal plane of the finite strain ellipsoid in a non-coaxial deformation. Consequently shearing along a P-domain is possible. In an anastomosing foliation, it is to be expected that some P-domains will have a component of shear stress along them whereas others will not.

In the former P-domains any widening of the lamellae and growth of phyllosilicates within the domains would have occurred during the shearing; a grain tending to grow across such a P-domain would be rotated into parallelism with the domain edges resulting in a deformed microstructure. In the latter case, if the P-domain was parallel to the x–y plane or if protected by being wholly confined within a Q-domain and if it remained in either

situation throughout the deformation then sliding would not occur. New phyllosilicate grains which were initially at an angle to the cleavage would be free to grow across the P-domain; that is, an annealed texture results. Furthermore, grains would be expected to grow across the P-domain/Q-domain contacts. However, as these show no signs of being deformed after entering a Q-domain it appears that grain growth continued after deformation. This may also explain the rarity of sandwich structures (as described by White & Knipe (1978) in their study of the Rhosneiger slates) in the P-domains.

The cataclasitic textures in the P-domains penetrating the silty layers do not show evidence for healing; no new phyllosilicates were seen growing in the shredded phyllosilicates and no corrosion of the microfractures or rounding of fragments were seen in quartz grains. These features would be expected if pressure solution processes were operative (Rutter & White 1979). The intrafolial nature of the bending of phyllosilicates again suggests that sliding had occurred along these P-domains, but that the sliding was late, when the rocks were in a 'dry' condition. This may be evidence for slight deformation during uplift.

The total amount of sliding, i.e. both the syn- and post-cleavage sliding, was not great as there is little obvious displacement of the silty layers and is more likely to be on the scale of microns rather than millimetres. However, a displacement of 1 μm on each penetrative domain, which has a spacing of about 25 μm would result in a total sliding displacement of 4 cm per metre width of slate.

Chemical changes in the phyllosilicates

Chemical changes in the phyllosilicates accompanied their re-orientation by crystallization into P-domains. The micas became more phengitic in content and the chlorites were enriched in Al but depleted in Fe. These trends were independent of the size and microstructural type of all P-domains, and are similar to those reported by Knipe (1979) for the Rhosneigr slates and for the nearby Clunes slate (Stephens *et al.* 1979). Detailed comparisons between this latter slate and that reported in this paper show almost identical trends. If anything they appear sharper in the Wattle Gully slates but this is more likely to reflect the different analytical techniques used. The STEM enabled us to separate P- and Q-domain phyllosilicates, especially in Q-domains where small P-domains with a width below the resolution of an optical microscope were common. The composition of the P-domain grains appear to be equilibrating to new PT conditions; similar trends in phengite composition have been reported with increasing metamorphic grade (Dunoyer de Segonzac 1970, Guidotti 1973), although this is a controversial matter with several authors reporting effectively the opposite trend, e.g. an increase in Al content with temperature (Butler 1965, Kwak 1968, Wenk 1970), a decrease in Si (Brown 1968) or a decrease in the ratio Si^{4+}/Al^{IV} (Cipriani *et al.* 1971).

The differences in P- and Q-domain phyllosilicate compositions do show, as stressed by Stephens *et al.* (1979), that limited ion exchange has occurred between the old grains and the fluids. This is all the more surprising when it is considered that sufficient solid state diffusion occurred to allow grain growth and the development of the annealed texture of some P-domains as well as the interpenetrating growth of phyllosilicates across P- and Q-domain contacts.

CONCLUSIONS

(1) The cleavage in the slate studied developed from pre-existing microcrenulations mainly by crystallization processes which were supported by pressure solution and mechanical rotation.

(2) The micas and chlorites in the P- and Q-domains had different mineral chemistries. Those in the P-domains were consistent with equilibration to a higher metamorphic temperature. In other words, those in the Q-domains reflected diagenesis and those in the P-domains, low grade metamorphism. The composition of the Q-domain phyllosilicates had not equilibrated with fluids flowing through the slate during foliation development.

(3) The P-domains exhibited two types of microstructure—deformed and annealed. The former is thought to reflect shearing during foliation development whereas the latter were parallel to the xy plane of the finite strain ellipsoid.

(4) A late shearing occurred along some of the lamellae resulting in the development of a catalastic microstructure.

Acknowledgements—Dr. O. P. Singleton, University of Melbourne, and the management of the Wattle Gully Gold Mine are thanked for their help in obtaining specimens. The research was financed by NERC grant GR3 3848. Dr. R. J. Knipe is thanked for the analysed standard mica sample. The paper also benefited greatly from the constructive criticisms of two reviewers.

REFERENCES

Bayly, B. M., Borradaile, G. S. & Powell, C. McA. 1977. *Atlas of Rock Cleavage*. Univ. of Tasmania Press, Tasmania.

Beach, A. 1979. Pressure solution as a metamorphic process in deformed terrigenous sedimentary rocks. *Lithos* **12**, 51–58.

Beavis, F. C. 1976. Structures in the Ordovician rocks of Victoria. *Proc. R. Soc. Vict.* **80**, 147–182.

Brown, E. H. 1968. The Si^{4+} content of natural phengites: a discussion. *Contr. Miner. Petrol.* **17**, 78–81.

Butler, B. C. M. 1965. Compositions of metamorphic micas. In: *Controls of Metamorphism* (edited by Pitcher, W. S. & Flinn, G. W.), Liverpool, 291–298.

Cipriani, C., Sassi, F. P. & Scolari, A. 1971. Metamorphic white micas: a definition of paragenetic fields. *Schweiz. miner. petrogr. Mitt.* **51**, 259–303.

Cliff, G. & Lorrimer, G. W. 1975. The quantitative analysis of thin specimens. *J. Microscopy* **103**, 203–207.

Craw, D. 1981. Oxidation and microprobe-induced potassium mobility in iron-bearing phyllosilicates from the Otago schists, New Zealand. *Lithos* **14**, 49–58.

Dunoyer de Segonzac, 1970. The transformation of clay minerals during diagenesis and low-grade metamorphism: a review. *Sedimentology* **15**, 281–346.

Geiser, P. A. 1975. Slaty cleavage and the dewatering hypothesis—an examination of some critical evidence. *Geology* **3**, 717–720.

Glasson, M. J. & Keays, R. R. 1978. Gold mobilization during cleavage

development in sedimentary rocks from the auriferous slate belt of Central Victoria, Australia: Some important boundary conditions. *Econ. Geol.* **73,** 496–511.

Goodhew, P. J. & Chescoe, D. 1980. Microanalysis in the transmission electron microscope. *Micron* **11,** 153–181.

Grant, P. R. & White, S. H. 1978. Cathodoluminescence and microstructure of quartz overgrowths on quartz: *Scanning Electron Microscopy* 1978 I SEM Inc., AMF O'Hare, Ill. 60666, U.S.A., 789–793.

Gray, D. R. 1977. Mrophologic classification of crenulation cleavage. *J. Geol.* **85,** 229–235.

Groshong, R. N. 1975. Strain, fractures and pressure solution in natural single folds. *Bull. geol. Soc. Am.* **86,** 1363–1376.

Guidotti, C. V. 1973. Compositional variation of muscovite as a function of metamorphic grade and assemblage in metapelites from N.W. Maine. *Contr. Miner. Petrol.* **42,** 33–42.

Knipe, R. J. 1979. Chemical changes during slaty cleavage development. *Bull. Miner.* **102,** 206–210.

Knipe, R. J. & White, S. H. 1977. Microstructural variation of an axial plane cleavage around a fold—a HVEM study. *Tectonophysics* **39,** 355–381.

Kwak, T. A. P. 1968. Ti in biotite and muscovite as an indicator of metamorphic grade in almandine amphibolite facies rocks from Sudbury, Ontario. *Geochim. cosmochim. Acta* **32,** 1222–1228.

Lorrimer, G. W., Razik, N. A. & Cliff, G. 1973. The use of the analytical electron microscope EMMA-4 to study the solute distribution in thin foils: some applications to metals and minerals. *J. Microscopy* **99,** 153–164.

Oertal, G. & Phakey, P. P. 1972. The texture of a slate from Nantlle, Caernarvon, North Wales. *Texture* **1,** 1–8.

Rutter, E. H. & White, S. H. 1979. The microstructures and rheology of fault gouges produced experimentally under wet and dry conditions at temperatures up to 400°C. *Bull. Miner.* **102,** 101–109.

Stephens, M. B., Glasson, M. J. & Keays, R. R. 1979. Structural and chemical aspects of metamorphic layering development in metasediments from Clunes, Australia. *Am. J. Sci.* **279,** 129–160.

Wenk, E. 1970. Distribution of Al between coexisting micas in metamorphic rocks from the Central Alps. *Contr. Miner. Petrol.* **26,** 50–61.

White, S. H. & Knipe, R. J. 1978. Microstructure and cleavage development in selected slates. *Contr. Miner. Petrol.* **66,** 165–174.